Vol 14 No 9, September 2005
1009-1963/2005/14(09)/1896-04

Chinese Physics

© 2005 Chin. Phys. Soc.
and IOP Publishing Ltd

Floating zone growth and magnetic and specific heat properties of $La_{0.67}Ca_{0.33}Mn_{1-x}Fe_xO_3$ (x=0.00, 0.04) single crystals

Kou Zhi-Qi(寇志起)†, Ma Xiao(马 骁), Di Nai-Li(邸乃力),
Li Qing-An(李庆安), and Cheng Zhao-Hua(成昭华)

State Key Laboratory of Magnetism, Institute of Physics, Chinese Academy of Sciences, Beijing 100080, *China*

(Received 16 March 2005; revised manuscript received 25 May 2005)

Single crystals of $La_{0.67}Ca_{0.33}MnO_3$ and $La_{0.67}Ca_{0.33}Mn_{0.96}Fe_{0.04}O_3$ were obtained by floating zone method. Laue diffraction pattern and rocking curve of the single crystals show that their quality is good. The magnetic behaviours of these compounds have been studied. Fe doping significantly depresses the magnetic contribution to the total specific heat C_P, but slightly influences the lattice contribution at temperatures above 50K. The peak of C_P shifts towards high temperatures with increasing magnetic field. Both single crystals exhibit the first-order magnetic transition around the Curie temperature.

Keywords: perovskite manganite, floating zone method, specific heat
PACC: 8110H, 7540C, 7530V

1. Introduction

Since the discovery of the colossal magnetoresistance (CMR) effect in perovskite rare earth manganites,[1] great effort has been made to understand their basic principle.[2,3] General formula of manganites exhibiting CMR is $Ln_{1-x}A_xMnO_3$, where A is a divalent ion substituting for Ln. Many authors have reported on significant differences between single crystals and polycrystalline samples of manganites. Single crystals exhibit much higher CMR than polycrystalline samples at temperatures just below the transition to the metallic state. There are several reports on single crystal growth of A-site doping,[4−6] but the reports for B-site doped single crystal growth are relatively rare.[7] Since the basic understanding of the CMR effect has a great impact on the potential application of these materials, high-quality single crystals are needed for the study of their intrinsic properties. So we describe the growth of $La_{0.67}Ca_{0.33}Mn_{0.96}Fe_{0.04}O_3$ single crystal in detail in this paper and compare the magnetic and specific heat properties of it with those of $La_{0.67}Ca_{0.33}MnO_3$ single crystal.

2. Experimental procedures

The single crystals were grown through the floating-zone method (FZM) with four ellipsoidal mirrors (Crystal Systems Inc, FZ-T-10000-H-VI-VP). Polycrystalline samples with nominal compositions of $La_{0.67}Ca_{0.33}MnO_3$ and $La_{0.67}Ca_{0.33}Mn_{0.96}Fe_{0.04}O_3$ were prepared by the standard solid-state reaction. The raw materials (La_2O_3, $CaCO_3$, $MnCO_3$ and Fe_2O_3 with 99.99% purity) were weighed after pretreatment and mixed in an agate mortar, then palletized and sintered at 1573K for 30h in mixed atmosphere of 50% Ar and 50% O_2. The structure and phase purity of the polycrystalline samples were checked by a Rigaku x-ray diffractometer with a rotating anode and Cu Kα radiation. The x-ray diffraction (XRD) patterns proved that these two samples are single phase of a perovskite-like structure. Then the polycrystalline pallets were ground to powder again and compressed hydrostatically in a rubber tube into rods with a diameter of 8mm and a length of 60mm. These rods were heated in mixed atmosphere at 1723K for 100h to form polycrystalline rods. Two of the sintered rods served as the seed and feed rods, which rotated at ∼28rpm in opposite directions. When we

†E-mail: kouzq@aphy.iphy.ac.cn

grew single crystal, the feed rod at first time at a low speed, the bottom of the feed rod became stacking, cracking and collapsing because the sintering temperature of the feed rod is not so high, so that the density is not high enough. The other reason for cracking was due to the composition gradients of calcium between the molten part and the crystal. The expansion of domains with slightly different lattice constants caused cracks. So we first pre-grew the sample at the fastest speed in order to make the feed rod dense enough, and then grew it stably at a speed of 1.5–2.5mm/h in the second time. This method is effective for preventing cracking and collapsing.

3. Results and discussion

Figure 1 presents a typical crystal boule grown at a speed of 2mm/h. The boules are all black with a metallic luster. The diameter of our samples is about 6–7mm, and the length is about 20–30mm. We used the inductively coupled plasma atomic emission spectroscopy (ICP-AES) to determine the compositions of our single crystals. For this kind of material, it is difficult to obtain homogeneous calcium content across the whole crystal. For example, for a single crystal without Fe doping, the concentration of calcium on the bottom of the crystal is about 0.34 and decreases by 0.001/mm gradually with growing process. This happens because the effective distribution coefficient for calcium is $K_{\mathrm{Ca}} = C_{\mathrm{s}}/C_{\mathrm{m}} < 1$, where C_{s} and C_{m} are the cation concentrations in the solid and the melt, respectively. As the solidification is carried on, there is an increase in the calcium content in the melt (due to the Ca segregation). But Cadoso *et al* [8] considered that there is an equilibrium point where the crystal became homogeneous with respect to calcium content because the amount of calcium going from the solid state to the molten zone becomes equal to the amount of calcium incorporated into the crystal. The compositions at the middle of the two sample crystals ($La_{0.69}Ca_{0.31}MnO_3$ (LCMO) and $La_{0.68}Ca_{0.32}Mn_{0.96}Fe_{0.04}O_3$ (LCMFO)) were determined.

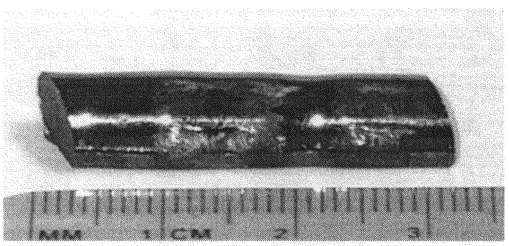


Fig.1. LCMO single crystal grown by FZM.

XRD experiment was carried out to check the single crystal and determine the crystallographic direction. Figure 2(a) shows the back-reflection Laue diffraction pattern of LCMFO, which is in the [00l] direction with a four-fold symmetry. XRD pattern and rocking curve of the LCMFO single crystal along [00l] direction measured by a Rigaku x-ray diffractometer are given in Fig.2(b). The rocking curve of (004) Bragg-reflection peak shows a FWHM of 0.4°, suggesting a high quality of the single crystal. Laue diffraction pattern and rocking curve of LCMO are similar to that of LCMFO in the same direction.

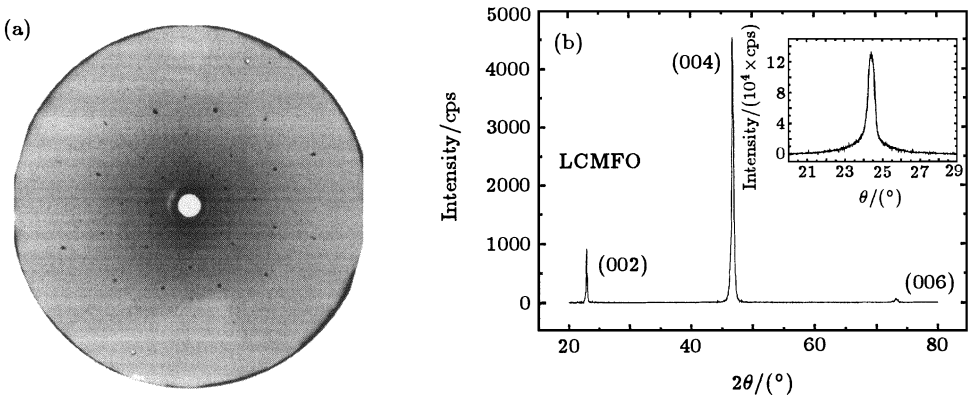


Fig.2. Laue diffraction (a) and x-ray diffraction (b) pattern of LCMFO single crystal along the [00l] direction. The inset shows the rocking curve of (004) Bragg-reflection peak for LCMFO single crystal.

Magnetization and specific heat measurements were performed on a commercial physical property measurement system (Quantum Design, PPMS-14). Magnetic fields are parallel to the long axis of the sample ([00l] direction). Figure 3 shows the temperature and magnetic field dependence of the DC susceptibility M for LCMO and LCMFO under a 0.16×10^5A/m magnetic field. The Curie temperature T_C is about 218K for LCMO and 174K for LCMFO, where a paramagnetic (PM) to ferromagnetic (FM) transition happens. Inset of Fig.3 shows that the saturation magnetic field is about 4.8×10^5A/m for LCMFO at 5K.

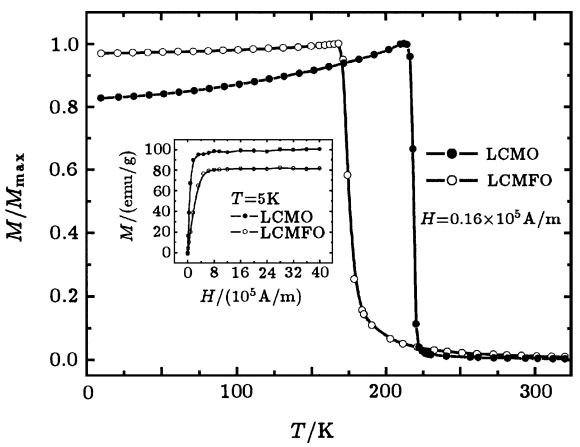


Fig.3. Temperature dependence of DC susceptibility measured at H=0.16×10^{5}A/m for LCMO and LCMFO. The inset shows the magnetic field dependence of magnetization at 5K.

Figure 4 displays the specific heat of LCMFO as a function of temperature above 50K under zero magnetic field. A sharp peak of the specific heat appears around the Curie temperature. We use three-optical-phonon Einstein model to evaluate the phonon contribution $C_{\rm phonon}$,[9]

$$C_{\rm Einstein} = 3rR\sum_i a_i[x_i^2{\rm e}^{x_i}/({\rm e}^{x_i}-1)^2],$$

where $x_i = h\upsilon_i/k_{\rm B}T$ (i=1, 2, 3), $k_{\rm B}$ is Boltzmann's constant, r=5 is the number of atoms per ABO_3 unit cell, and R is the gas constant. In this model, all the independent oscillators populate on the three optical modes of the frequencies of υ_i in the ratio of $a_1 : a_2 : a_3$. The fitting of experimental data to this equation gives the Einstein modes of $h\upsilon_i/k_{\rm B}$=138, 423, 985K and $a_1 : a_2 : a_3$= 2 : 7 : 1. Subtracting this phonon contribution $C_{\rm phonon}$ from the total specific heat $C_{\rm P}$, we obtain magnetic contribution to specific heat, $C_{\rm mag}$, and the results are shown in Fig.5. In contrast to $La_{0.7}Sr_{0.3}MnO_3$, of which the magnetic peak broadens and decreases in height without change with temperature under an applied field.[10] The magnetic fields drive the $C_{\rm mag}$ peak to high temperatures and depress its height for LCMO and LCMFO. Both LCMO and LCMFO exhibit the first-order magnetic transition around the Curie temperature. Fe doping decreases the Curie temperature by affecting the double exchange interaction of Mn^{3+} and Mn^{4+} ions.

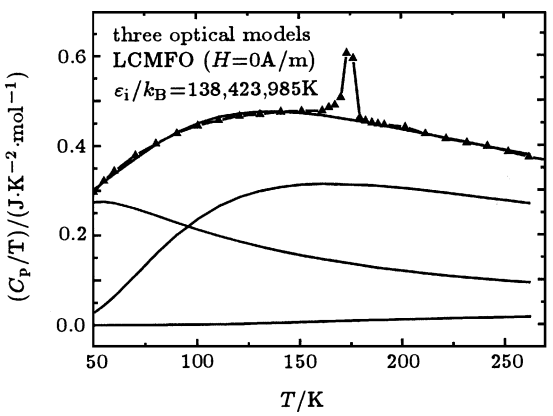


Fig.4. Specific heat of LCMFO under zero magnetic field. Solid lines are the results of curve fitting to three Einstein modes.

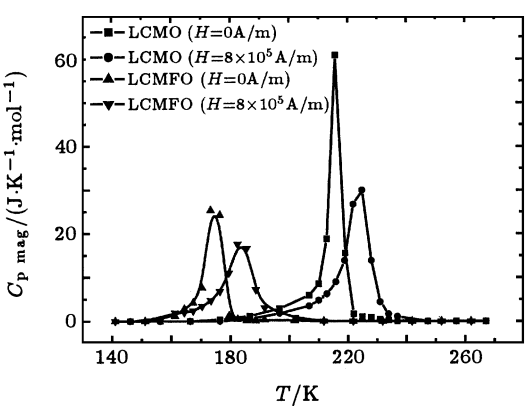


Fig.5. Temperature dependence of the magnetic contribution to specific heat of LCMO and LCMFO obtained under H=0 and 8×10^{5}A/m.

4. Conclusion

In conclusion, we have successfully grown the LCMO and LCMFO single crystals by the floating zone method. The stable growth of the single crystal is obtained by first growing fast, which can make the feed rod dense, then slowly. The crystal quality was checked by the rocking curve and back-reflection Laue diffraction. Magnetic and specific-heat properties show that both crystals experience a first-order

magnetic transition around the Curie temperatures. The incorporation of Fe atoms depresses significantly the magnetic contribution to the total specific heat, but influences the lattice contribution slightly.

References

[1] von Helmolt R, Wecker J, Holzapfel B, Schultz L and Samwer K 1993 *Phys. Rev. Lett.* **71** 2331

[2] Li R W, Wang Zh H, Chen X and Shen B G 1999 *Acta Phys. Sin.* **48** S105 (in Chinese)

[3] Lu Y, Li Q A, Di N L, Ma X, Kou Zh Q, Luo Zh and Cheng Zh H 2003 *Chin. Phys.* **12** 789

[4] Kloc Ch, Cheong S W and Matl P 1998 *J. Crystal Growth* **191** 294

[5] Shulyatev D, Karabashev S, Arsenov A and Mukovskii Ya 1999 *J. Crystal Growth* **198** 511

[6] Shulyatev D, Karabashev S, Arsenov A, Mukovskii Ya and Zverkov S 2002 *J. Crystal Growth* **237** 810

[7] Takeuchi Jun, Dhakal Tara P, Hirahara Seitaro and Miyoshi Kiyotaka 2002 *J. Magn. Magn. Mater.* **239** 173

[8] Cardoso C A, Araujo-Moreira F M, Andreeta M R B, Hernandes A C, Leite E R, de Lima O F, Mombru A W and Faccio R 2003 *Appl. Phys. Lett.* **83** 3135

[9] Raychaudhuri A K, Guha Ayan, Das I, Rawat R and Rao C N R 2001 *Phys. Rev.* B **64** 165111

[10] Lin P, Chun S H, Salamon M B, Tomioka Y and Tokura Y 2000 *J. Appl. Phys.* **87** 5825